



UNIVERSITY OF LEEDS

This is a repository copy of *MISO Model Free Adaptive Control of Single Joint Rehabilitation Robot Driven by Pneumatic Artificial Muscles**.

White Rose Research Online URL for this paper:

<https://eprints.whiterose.ac.uk/165852/>

Version: Accepted Version

Proceedings Paper:

Li, Y, Liu, Q, Meng, W et al. (3 more authors) (2020) MISO Model Free Adaptive Control of Single Joint Rehabilitation Robot Driven by Pneumatic Artificial Muscles*. In: 2020 IEEE/ASME International Conference on Advanced Intelligent Mechatronics (AIM). 2020 IEEE/ASME International Conference on Advanced Intelligent Mechatronics (AIM), 06-09 Jul 2020, Boston, Massachusetts, USA. IEEE , pp. 1700-1705. ISBN 978-1-7281-6795-4

<https://doi.org/10.1109/aim43001.2020.9158805>

Reuse

Items deposited in White Rose Research Online are protected by copyright, with all rights reserved unless indicated otherwise. They may be downloaded and/or printed for private study, or other acts as permitted by national copyright laws. The publisher or other rights holders may allow further reproduction and re-use of the full text version. This is indicated by the licence information on the White Rose Research Online record for the item.

Takedown

If you consider content in White Rose Research Online to be in breach of UK law, please notify us by emailing eprints@whiterose.ac.uk including the URL of the record and the reason for the withdrawal request.



eprints@whiterose.ac.uk
<https://eprints.whiterose.ac.uk/>

MISO Model Free Adaptive Control of Single Joint Rehabilitation Robot Driven by Pneumatic Artificial Muscles*

Yi Li, Quan Liu, Wei Meng, *Member, IEEE*, Yuanlong Xie, Qingsong Ai, *Member, IEEE*, Sheng Q Xie, *Senior Member, IEEE*

Abstract— Pneumatic artificial muscles (PAMs) are widely used as actuators in the field of rehabilitation robots, but their intrinsic compliance properties make it difficult to control precisely. In this paper, an improved multiple input single output model free adaptive control (MISO-IMFAC) method is proposed for the modeling the uncertainty, high nonlinearity and time-variability of the single joint rehabilitation robot driven by antagonistic PAMs, so as to realize the high-precision control of the joint angle. Considering the influence of the error change of adjacent time on the actual control effect, a new control law is formed by adding a term representing error change to the original control input criterion function. The experiment is carried out on a real rehabilitation robot and four types of errors are used to evaluate the effectiveness of the control system. The results show that the control algorithm can improve the accuracy of angle trajectory tracking at different amplitudes. Compared with original algorithm, the experiment errors of MISO-IMFAC were significantly reduced. In addition, the MISO-IMFAC still maintains stable performance in the process of load variation and external disturbance.

I. INTRODUCTION

With the improvement of people's living standards, the incidence of cardiovascular diseases also increases. According to the world health organization (WHO), among the top 10 causes of death in the world in 2016, stroke ranks the second, becoming the biggest killer following ischaemic heart disease [1]. Rehabilitation after stroke has become a problem worthy of attention. The use of rehabilitation robots helps patients recover more quickly from the injury after stroke [2]. In fact, the robot can provide long-term and quantitative rehabilitation treatment for patients, which is similar to the treatment effect provided by therapists, and the use of sensors also makes real-time monitoring possible. The

evaluation becomes convenient, at the same time, there is also a basis for the next rehabilitation program [3].

Rigid actuators have the possibility to cause secondary damage to the human body, which is detrimental to the patient's recovery [4]. Compared with rigid motors, pneumatic artificial muscles (PAMs) are more compliant and safer. The use of them as actuators meets the requirements of safety, softness and comfort during the rehabilitation process. The structure of the single joint rehabilitation robot driven by PAMs is not complicated. On the one hand, the driving method determines that the robot has the same advantages as the PAMs. On the other hand, the similarity of human joints makes the robot suitable for the rehabilitation of elbow, knee and any other limb joint, which can greatly improve the utilization rate of equipment.

However, the special structure of PAMs determine that they have nonlinear and time-varying characteristics, which makes it very difficult to control the robot driven by PAMs [5]. A large number of people have been involved in related research, using different control methods to control PAM and the robot driven by PAMs. Taking PAM as the control object, Chen et al. [6] proposed a T-S fuzzy logic control method based on genetic algorithm optimization. The experimental results show that this method can achieve ideal control performance, and has the ability to improve control accuracy while overcoming the jitter phenomenon of trajectory tracking. Liu et al. [7] designed PID and two kinds of novel sliding mode control methods. The experimental results show that the novel sliding mode control method has more superior performance in the position control of PAM. Considering the characteristics of the exoskeleton rehabilitation robot driven by PAMs, Tu et al. [8] used iterative learning control to control the newly designed rehabilitation system, and the robot realized repetitive task training for patients. Zhong et al. [9] designed an adaptive controller based on BPNN, which can track the position of PAM accurately. In addition, due to the different advantages and disadvantages of different control methods, there are also examples of combining various control algorithms to control PAMs [10, 11].

Model free adaptive control (MFAC) algorithm is a control algorithm that does not need any model information of the controlled system and has better robustness than model-based control algorithm [12]. Compared with other model free control methods, MFAC algorithm has the following advantages. The training of neural network model needs huge data, so it is a challenge for data acquisition and processing [13]. PID control belongs to the category of model free control, but for the system of high nonlinearity and time-variability, the effect of PID control is not ideal [14].

*Research supported by National Natural Science Foundation of China under grant numbers 51705381 and 51675389 and the Key Program for International S&T Cooperation of Hubei Province under 2018AHB007, also supported by the Fundamental Research Funds for the Central Universities (WUT: 2020III024GX). (*Corresponding author: Wei Meng*)

Y. Li is with School of Information Engineering, Wuhan University of Technology, 122 Luoshi Road, Wuhan, China (yili1995@whut.edu.cn).

Q. Liu is with the School of Information Engineering, Wuhan University of Technology, 122 Luoshi Road, Wuhan (quanliu@whut.edu.cn).

W. Meng is with the School of Information Engineering, Wuhan University of Technology, 122 Luoshi Road, Wuhan, China and the School of Electronic and Electrical Engineering, University of Leeds, Leeds, LS2 9JT, UK (email: weimeng@whut.edu.cn, w.meng@leeds.ac.uk).

Y. Xie is with the School of Mechanical Science and Engineering, Huazhong University of Science and Technology, Wuhan, China.

Q. Ai is with the School of Information Engineering, Wuhan University of Technology, 122 Luoshi Road, Wuhan (qingsongai@whut.edu.cn).

S. Q. Xie is with the School of Electronic and Electrical Engineering, University of Leeds, Leeds, LS2 9JT, UK (email: s.q.xie@leeds.ac.uk).

MFAC algorithm has a variety of dynamic linearization forms including compact format, which is suitable for various systems, such as single input single output (SISO), multiple input single output (MISO), and multiple input multiple output (MIMO). The original algorithm and the improved algorithm have been used to solve the control problems of various real systems. Liu et al. [15] applied a new MFAC algorithm based on a dual successive projection to automatic driving to realize lateral tracking control during the driving of the vehicle. When the speed was 5km/h and 10km/h, the RMSE of MFAC was 0.1320 and 0.1472, respectively, which were far lower than the traditional PID algorithm. Li et al. [16] proposed a control scheme based on MFAC to solve the problem of flexible integrated joint force control for collaborative robots. The control method has the characteristics of time-varying and uncertainty, which can achieve high control performance. Based on the MFAC method of MIMO nonlinear system, the data-driven formation control of nonlinear multi-agent system is realized by Zhang et al. [17] The simulation results show the effectiveness of MFAC method.

Considering the nonlinear and time-varying characteristics of the single joint rehabilitation robot, this paper proposes an improved multiple input single output model free adaptive control (MISO-IMFAC) system to improve the accuracy of angle control of the joint platform, and the experimental results show the effectiveness of this method. The rest of this paper is organized as follows: Section II introduces motion principle and design of the single joint rehabilitation robot and its mathematical expression of kinematics and dynamics. Section III designs the control system. In Section IV, the actual control experiment is carried out and the results are obtained. Then the conclusion is given in Section V.

II. SINGLE JOINT REHABILITATION ROBOT

A. Robot Design

PAM is a new type of actuator which can only contract. When the PAM is inflated, under the action of air pressure, it expands radially, resulting in its axial contraction. On the contrary, when the PAM is deflated, it stretches axially, at which time its length increases. The single joint rehabilitation robot is driven by a pair of antagonistic PAMs, as shown in Figure 1. This form is called pulley type. Besides, there are lever type [18] and pendulum type [19]. Figure 1(a) shows the initial state of the single joint rehabilitation robot. In this state, the pair of antagonistic PAMs are inflated and contracted to half of the contractible maximum length. When the robot is in working state, as shown in Figure 1(b), the PAMs on both sides are alternately inflated and deflated and the joint starts to rotate under the action of the rope. At this time, the connecting rod drives the patient's limb for rehabilitation training.

B. Kinematics and Dynamics

When the initial joint angle is defined as 0 degree, the kinematic equation can be expressed by (1).

$$\theta = \frac{L_0 - L_1}{2\pi R} \times 360 \quad (1)$$

where θ is the joint angle, L_0 is the length of the single

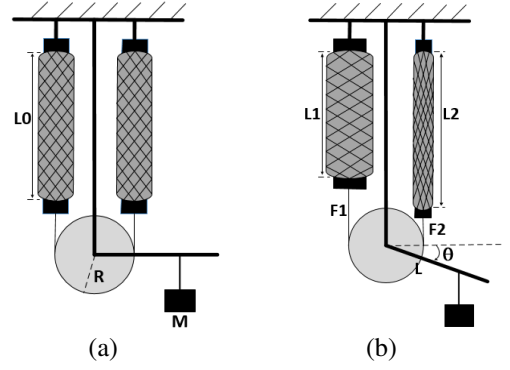


Figure 1. Simplified diagram of the single joint rehabilitation robot: (a) the initial state (b) the working state

PAM in the initial state, L_1 is the length of the left PAM in the working state, and R is the joint radius of the pulley.

Because the length of PAMs always satisfy the following relationship: $L_1 + L_2 = 2L_0 = CONST$, where L_2 is the length of the right PAM in the working state, so the above formula can also be expressed by (2).

$$\theta = \frac{L_2 - L_0}{2\pi R} \times 360 \quad (2)$$

If the mass of the load is defined as M , the dynamic equation can be expressed by (3).

$$(F_1 - F_2)R + MgL\cos\theta = J\ddot{\theta} + B\dot{\theta} \quad (3)$$

where F_1 is the tension of the left PAM in the working state, F_2 is the tension of the right side, θ and $\dot{\theta}$ represent the first-order derivative and second-order derivative of the joint angle respectively, J is the inertia of joint motion, B is the joint damping coefficient, L is the distance from the action point of the load on the connecting rod to the center of rotation of the pulley joint.

III. CONTROL SYSTEM

A. MISO-MFAC Algorithm

MISO nonlinear discrete-time system can be expressed by (4).

$$\theta(k+1) = f(\theta(k), \theta(k-1), \dots, \theta(k-n_\theta), \mathbf{u}(k), \mathbf{u}(k-1), \dots, \mathbf{u}(k-n_u)) \quad (4)$$

where $\mathbf{u}(k) \in \mathbf{R}^m$, $\theta(k) \in \mathbf{R}^1$ respectively represents the input signal and the output signal at time k , and n_θ and n_u represent the system order respectively, both of which are positive integers. $f(\dots)$ represents the unknown nonlinear function.

Assumption I: each of the components of $f(\dots)$ has a continuous partial derivative for the control input $\mathbf{u}(k)$.

Assumption II: for any $k_1 \neq k_2$, $k_1 \geq 0$, $k_2 \geq 0$ and $\mathbf{u}(k_1) \neq \mathbf{u}(k_2)$, $|\theta(k_1+1) - \theta(k_2+1)| \leq b\|\mathbf{u}(k_1) - \mathbf{u}(k_2)\|$, where b is a positive constant.

In the case that the above two assumptions are satisfied, the MISO nonlinear discrete-time system is equivalent to

$$\Delta\theta(k+1) = \phi_c^T(k)\Delta\mathbf{u}(k) \quad (5)$$

where $\phi_c(k) = \begin{bmatrix} \varphi_1(k) \\ \varphi_2(k) \\ \vdots \\ \varphi_m(k) \end{bmatrix}$ represents the pseudo gradient

(PG) of the system, and $\Delta\theta(k+1) = \theta(k+1) - \theta(k)$, $\Delta\mathbf{u}(k) = \mathbf{u}(k) - \mathbf{u}(k-1)$. It should be noted that $\phi_c(k)$ is bounded for any k .

Consider the control input criterion function expressed by (6).

$$J(\mathbf{u}(k)) = |\theta_d(k+1) - \theta(k+1)|^2 + \lambda \|\mathbf{u}(k) - \mathbf{u}(k-1)\|^2 \quad (6)$$

where $\theta_d(k+1)$ represents the desired output at time $k+1$, and λ is the weight factor, which is positive.

Let $\frac{\partial J(\mathbf{u}(k))}{\partial \mathbf{u}(k)} = 0$, and we can get the equation (7).

$$\mathbf{u}(k) = \mathbf{u}(k-1) + \frac{\rho\phi_c(k)(\theta_d(k+1) - \theta(k))}{\lambda + \|\phi_c(k)\|^2} \quad (7)$$

where $0 < \rho \leq 1$ is the step factor, which can make the control algorithm more general.

$\phi_c(k)$ is a time-varying parameter, and its accurate value is difficult to obtain. Therefore, the following equation (8) is used to estimate the PG.

$$J(\hat{\phi}_c(k)) = \left| \Delta\theta(k) - \hat{\phi}_c^T(k)\Delta\mathbf{u}(k-1) \right|^2 + \mu \|\hat{\phi}_c(k) - \hat{\phi}_c(k-1)\|^2 \quad (8)$$

where μ is the weight factor, which is positive.

Let $\frac{\partial J(\hat{\phi}_c(k))}{\partial \hat{\phi}_c(k)} = 0$, and we can get the equation (9).

$$\hat{\phi}_c(k) = \hat{\phi}_c(k-1) + \frac{\eta \left(\Delta\theta(k) - \hat{\phi}_c^T(k-1)\Delta\mathbf{u}(k-1) \right) \Delta\mathbf{u}(k-1)}{\mu + \|\Delta\mathbf{u}(k-1)\|^2} \quad (9)$$

where $0 < \eta \leq 2$ is the step factor, and $\hat{\phi}_c(k) = \begin{bmatrix} \hat{\varphi}_1(k) \\ \hat{\varphi}_2(k) \\ \vdots \\ \hat{\varphi}_m(k) \end{bmatrix}$

is an estimate of $\phi_c(k)$.

In order to enhance the ability of the PG estimation algorithm to track time-varying parameters, the following reset mechanism needs to be introduced.

$$\hat{\varphi}_i(k) = \hat{\varphi}_i(1), \text{ if } \hat{\varphi}_i(k) < b \text{ or } \text{sign}(\hat{\varphi}_i(k)) \neq \text{sign}(\hat{\varphi}_i(1)), i = 1, \dots, m \quad (10)$$

Equations (7), (9) and (10) together constitute the MISO-MFAC scheme. It can be seen that this scheme only uses the input data and output data of the controlled system. According to the information of the actual output signal and the desired output signal, the scheme will automatically update the PG and input signal, so as to achieve the purpose of adaptive control. The PG is not sensitive to the time-delay

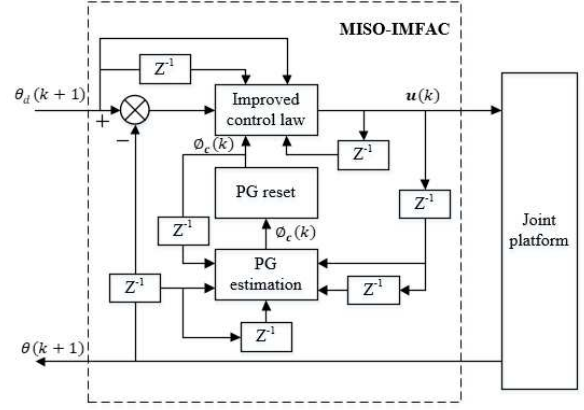


Figure 2. Structure diagram of MISO-IMFAC system for joint platform

and time-varying characteristics of the system, so the control scheme has strong adaptability and robustness.

B. MISO-IMFAC Algorithm

Proper usage of error information during control can improve the control accuracy [20], so we redefine the control input criterion function.

$$J(\mathbf{u}(k)) = Q_1|e(k+1)|^2 + Q_2|e(k+1) - e(k)|^2 + \lambda \|\mathbf{u}(k) - \mathbf{u}(k-1)\|^2 \quad (11)$$

where $e(k+1) = \theta_d(k+1) - \theta(k+1)$, and $Q_1, Q_2 > 0$. They are also called the weight factors.

Let $\frac{\partial J(\mathbf{u}(k))}{\partial \mathbf{u}(k)} = 0$, and we can get the equation (12).

$$\mathbf{u}(k) = \mathbf{u}(k-1) + \frac{\rho\phi_c(k) \left(Q_1(\theta_d(k+1) - \theta(k)) + Q_2(\theta_d(k+1) - \theta_d(k)) \right)}{\lambda + Q_1\|\phi_c(k)\|^2 + Q_2\|\phi_c(k)\|^2} \quad (12)$$

Therefore, equations (9), (10) and (12) together constitute the MISO-IMFAC scheme. In the control process, desired value, initial input and output signal, initial PG, and other parameters, including the weight factors and the step factors, need to be provided.

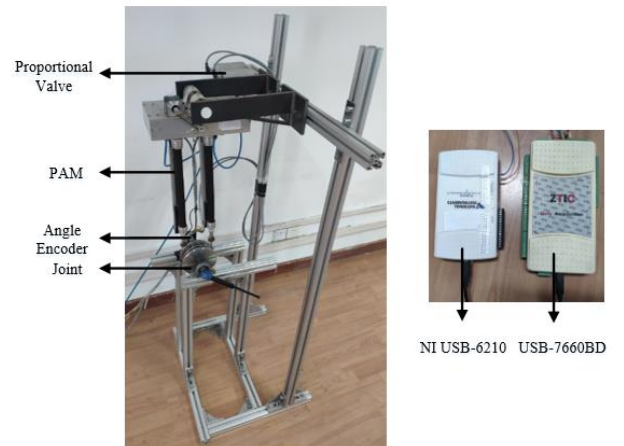


Figure 3. Experimental platform of the single joint rehabilitation robot

The single joint rehabilitation robot can be regarded as an MISO system. The input is the control signal of two PAMs, and the output is the joint angle. The designed MISO-IMFAC system for joint platform is shown in Figure 2. Starting from the actual angle and the desired angle, we can get $u(k)$ through three steps of the PG estimation, reset mechanism and acquisition of the control input. They correspond to equations (9), (10) and (12) respectively. Under the action of the control signal, the actual angle of the joint platform is obtained, so a closed loop is formed.

IV. EXPERIMENTS AND RESULTS DISCUSSION

A. Experimental Setup

Figure 3 shows the experimental platform of the single joint rehabilitation robot. The upper end of PAMs (FESTO MAS-20-400N) is fixed on a stable support, while the lower end is free, which is connected to the joint by ropes. The MISO-IMFAC program is written in LabVIEW. Control signal sent by the control program is converted into an analog signal by the data acquisition module (USB-7660BD) and sent to the proportional valve. Angle of the pulley joint is controlled by changing the air intake of the antagonistic PAMs. The angle encoder (XYK-BMJ-23Z4-V12) is located at the joint connecting rod. The measured angle signal is converted into digital value through the data acquisition device (NI USB-6210) and sent to the control program.

In order to better evaluate the effectiveness of the control system, four types of errors are defined below.

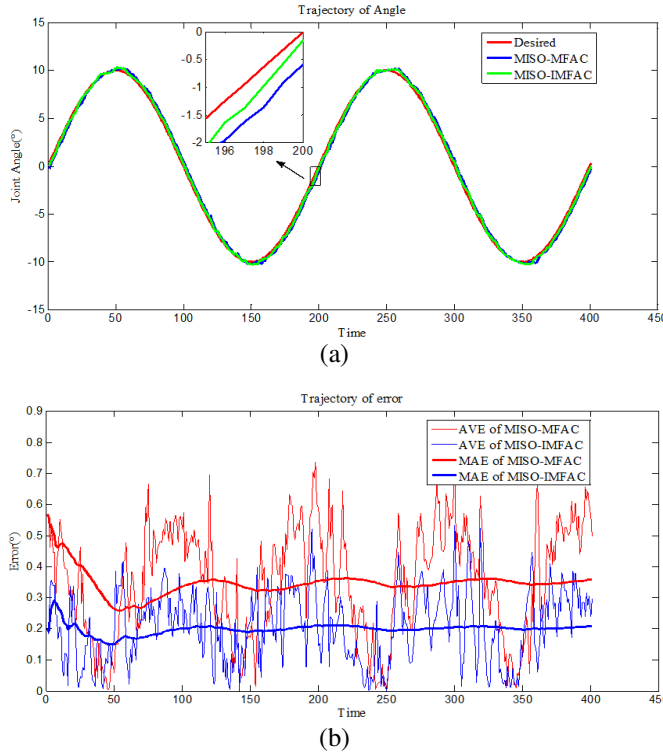


Figure 4. Angle trajectory tracking and error trajectory results (The desired angle amplitude =10°)

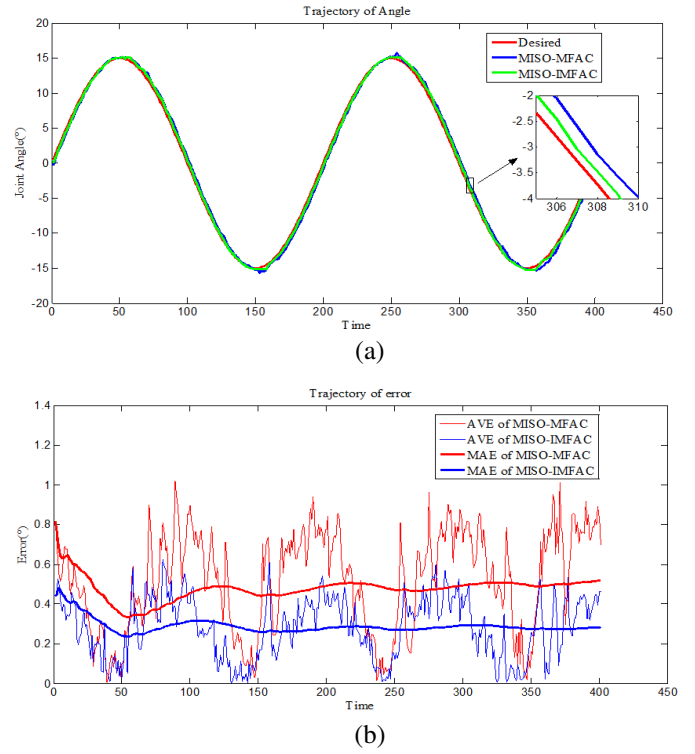


Figure 5. Angle trajectory tracking and error trajectory results (The desired angle amplitude =15°)

$$AVE = |\theta_d(k) - \theta(k)|, k = 1, 2, \dots, m$$

$$MAE = \frac{1}{m} \sum_{k=1}^m |\theta_d(k) - \theta(k)|$$

$$AVME = \max(|\theta_d(k) - \theta(k)|), k = 1, 2, \dots, m \quad (13)$$

$$RMSE = \frac{1}{m} \sum_{k=1}^m (\theta_d(k) - \theta(k))^2$$

where AVE is absolute value of error, MAE is mean absolute error, AVME is absolute value of maximum error, and RMSE is root mean square error.

B. Experimental Results

In order to ensure the effectiveness of rehabilitation training, it is necessary to control the angle of the joint accurately. In consideration of the need to ensure the smooth and slow motion and the suitability of the range of motion in the process of limb rehabilitation, the desired rotation angle is set as a sine curve with a frequency of 0.05Hz in this experiment. Under the condition of no load, the desired angle amplitude of the joint is 10°, 15° and 20° respectively. The results are shown in Figure 4, 5 and 6.

Figure 4, 5 and 6 show the angle trajectory and error trajectory when the desired angle amplitude is 10°, 15°, and 20°, respectively. In the angle trajectory curve, the red curve represents the desired angle of the joint. The control effects of the MISO-MFAC and MISO-IMFAC schemes are expressed by the blue curve and the green curve, respectively. Change the desired angle amplitude to get multiple effects. It can be seen from the experimental results that MISO-IMFAC has better control performance, which can be more clearly demonstrated after local magnification. The error trajectory

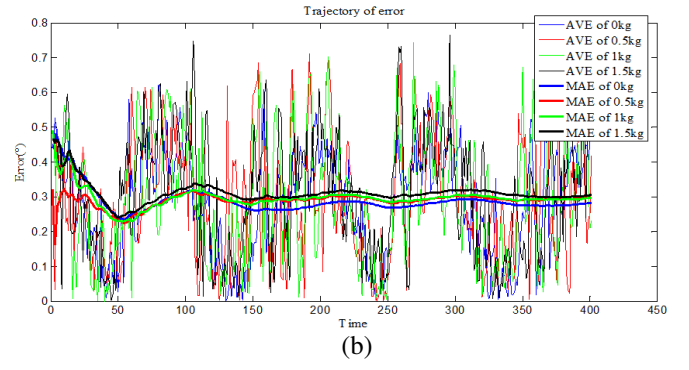
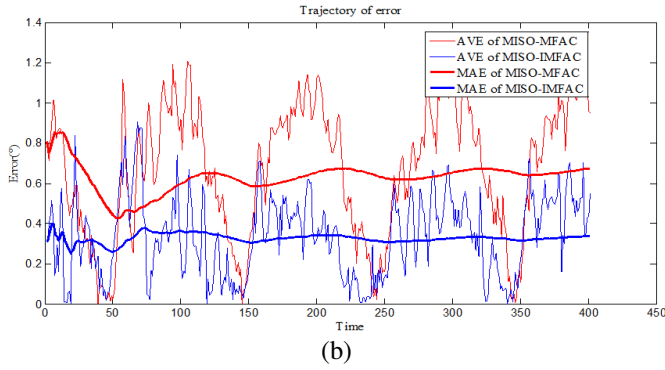
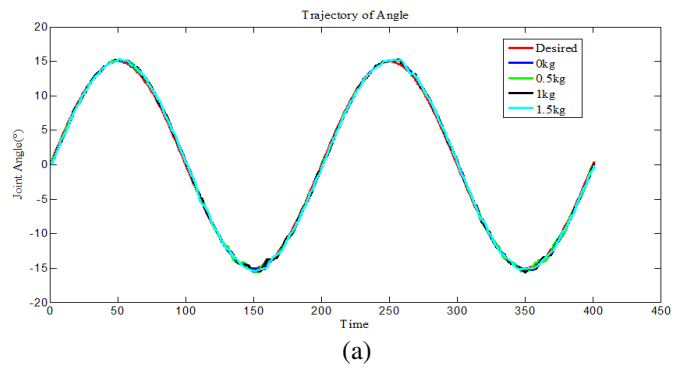
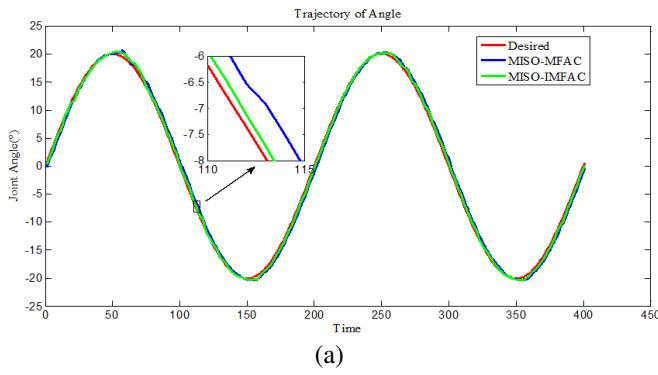


Figure 6. Angle trajectory tracking and error trajectory results (The desired angle amplitude =20°)

Figure 7. Angle trajectory tracking and error trajectory results under different loads

TABLE I. TRAJECTORY ERROR RESULTS FOR ANGLE

	Amplitude =10°		Amplitude =15°		Amplitude =20°	
	AVME	RMSE	AVME	RMSE	AVME	RMSE
MISO-MFAC	0.8044	0.0256	1.022	0.1102	1.3454	0.3146
MISO-IMFAC	0.5339	0.0032	0.6236	0.0107	0.9059	0.0244

TABLE II. TRAJECTORY ERROR RESULTS FOR ANGLE WHEN THE LOAD CHANGES

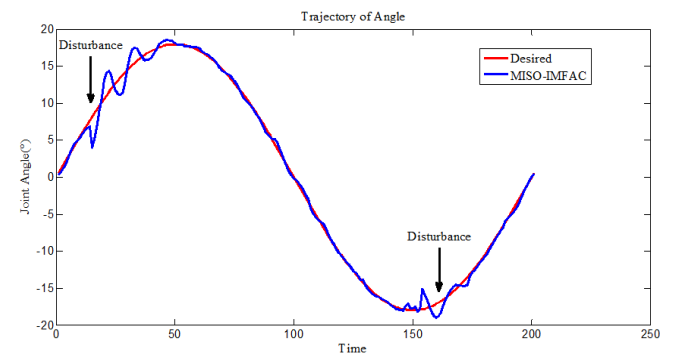
	load =0kg	load =0.5kg	load =1kg	load =1.5kg
AVME	0.6236	0.7129	0.7434	0.7657
RMSE	0.0107	0.0142	0.0145	0.0149

curve shows the AVE and MAE of the two algorithms. MISO-IMFAC are in lower position, indicating that the control effect of MISO-IMFAC is better than that of MISO-MFAC. Table I shows the effect of the two control methods from the perspective of data. Compared with MISO-MFAC, MISO-IMFAC decreased significantly in AVME and RMSE. Under different desired angle amplitudes of the joint, the reduction of AVME is more than 30% and the reduction of RMSE is more than 85%. In addition, it is worth mentioning that with the increase of the desired angle amplitude, the errors of both MISO-MFAC and MISO-IMFAC increase, which is also within the expectation.

illustrated by the AVE and MAE data. Actually, such results can be expected. As MISO-IMFAC is a data-driven control method and does not rely on the system model, the change in the system model caused by the change in load does not have a large impact on the control effect. The numerical results shown in table II illustrate this point more specifically. Let's explain it in two sets of numbers. When the load mass increases from 1kg to 1.5kg, AVME changes from 0.7434 to 0.7657, and RMSE from 0.0145 to 0.0149. Their rates of change are only 3.00% and 2.76%, respectively.

In this experiment, the pulley joint is connected to the rod, on which a weight is suspended, which can be similar to the contact between the connecting rod and the limb of the patient. By changing the mass of the load, the limb weight of different patients is simulated. In the experiment, four sets of control experiments were performed using the MISO-IMFAC scheme. The weight was 0kg, 0.5kg, 1kg and 1.5kg, and the desired angle amplitude of the whole process is guaranteed to be 15 degrees. The results are shown in Figure 7.

During the operation of the rehabilitation robot, there may



After changing the mass of the load, the actual angle trajectory curve does not change significantly, which is also

Figure 8. Tracking results of angle trajectory under external disturbance

be external disturbances. To verify that the designed control scheme has strong stability and anti-interference ability, an angle tracking experiment under external disturbances was also performed. As shown in Figure 8, the disturbance is artificially added at two moments when the peak is about to be reached and the rise starts from the trough. It should be noted that the experiment was performed under the condition of a desired angle amplitude of 18 degrees and no load.

At the moment when external disturbance was added, the actual angle oscillated to a certain extent, and the maximum errors were 4.17 and 2.76, respectively. Then, the oscillation gradually decreases until it returns to normal. The MISO-IMFAC method is characterized by strong stability and robustness, which can be well proved by this experiment.

V. DISCUSSION AND CONCLUSION

In this paper, a MISO-IMFAC method is proposed to control a single joint rehabilitation robot driven by PAMs. In the actual robot system, several experiments are carried out, including angle trajectory tracking under different desired amplitude, different load, and different external disturbance. The results show that the improved method has good tracking performance for joint angles. Compared with the original MISO-MFAC, the errors of MISO-IMFAC are significantly reduced under different desired angle amplitudes, among which the reduction of AVME is more than 30% and RMSE is more than 85%. The load variation and external disturbance experiments prove the stability and effectiveness of the designed controller. MISO-IMFAC is not sensitive to the change of load mass. Under the external disturbance, the curve can quickly return to normal and achieve accurate tracking. In the future, we intend to involve real patients. In addition, human-computer interaction with compliant and safe features and the modular design of robot software and hardware are also the focus of the next work.

REFERENCES

- [1] World Health Organization, "Global Health Estimates 2016: Deaths by Cause, Age, Sex, by Country and by Region, 2000-2016," <https://www.who.int/news-room/fact-sheets/detail/the-top-10-causes-of-death>, 2018.
- [2] H. Lee *et al.*, "Training for Walking Efficiency With a Wearable Hip-Assist Robot in Patients With Stroke: A Pilot Randomized Controlled Trial," *Stroke*, vol. 50, no. 12, pp. 3545-3552, 2019.
- [3] Y. Hung, P. Chen, and W. Lin, "Design factors and opportunities of rehabilitation robots in upper-limb training after stroke," in *international conference on ubiquitous robots and ambient intelligence*, 2017, pp. 650-654.
- [4] S. Guo, F. Zhao, W. Wei, J. Guo, X. Zhao, and W. Zhang, "Soft actuator for hand rehabilitation," in *international conference on mechatronics and automation*, 2015, pp. 2197-2202.
- [5] Q. Ai *et al.*, "High-Order Model-Free Adaptive Iterative Learning Control of Pneumatic Artificial Muscle with Enhanced Convergence," *IEEE Transactions on Industrial Electronics*, pp. 1-1, 2019.
- [6] C. Chen, J. Huang, D. Wu, and Z. Song, "T-S Fuzzy Logic Control with Genetic Algorithm Optimization for Pneumatic Muscle Actuator," in *International Conference on Modelling, Identification and Control (ICMIC)*, 2018.
- [7] H. Liu, Y. Zhao, F. Jiang, and X. Yao, "Pneumatic muscle actuator position control based on sliding mode control algorithms," in *international conference on information and automation*, 2015, pp. 1115-1120.
- [8] X. Tu *et al.*, "Iterative learning control applied to a hybrid rehabilitation exoskeleton system powered by PAM and FES," *Cluster Computing*, vol. 20, no. 4, pp. 2855-2868, 2017.
- [9] J. Zhong, X. Zhou, and M. J. C. Luo, "A New Approach to Modeling and Controlling a Pneumatic Muscle Actuator-Driven Setup Using Back Propagation Neural Networks," *Complexity*, vol. 2018, pp. 1-9, 2018.
- [10] C. Van Kien, T. T. Huan, D. T. Thai, and H. P. H. Anh, "Implementation of adaptive fuzzy sliding mode control for nonlinear uncertain serial pneumatic-artificial-muscle (PAM) robot system," in *international conference on system science and engineering*, 2017, pp. 83-88.
- [11] S. Boudoua, M. Hamerlain, and F. Hamerlain, "Intelligent Twisting Sliding Mode Controller using Neural Network for Pneumatic Artificial Muscles Robot Arm," in *International Workshop on Recent Advances in Sliding Modes*, 2015.
- [12] Z. Hou and Z. J. I. S. Wang, "From model-based control to data-driven control: Survey, classification and perspective," *Information Sciences*, vol. 235, no. 235, pp. 3-35, 2013.
- [13] H. Li *et al.*, "Fuzzy Optimized MFAC Based on ADRC in AUV Heading Control," *Electronics*, vol. 8, no. 6, pp. 608, 2019.
- [14] Z. Hou, R. Chi, and H. Gao, "An overview of dynamic-linearization-based data-driven control and applications," *IEEE Transactions on Industrial Electronics*, vol. 64, no. 5, pp. 4076-4090, 2017.
- [15] S. Liu, Z. Hou, T. Tian, Z. Deng, and Z. Li, "A Novel Dual Successive Projection-Based Model-Free Adaptive Control Method and Application to an Autonomous Car," *IEEE Transactions on Neural Networks and Learning Systems*, vol. 30, no. 11, pp. 3444-3457, 2019.
- [16] Y. Li, Y. Zhao, K. Li, Z. Wang, and X. Zhao, "Force Control of Flexible Integrated Joint Based on Model-free Adaptive Control," in *2018 IEEE International Conference on Robotics and Biomimetics*, 2018, pp. 1425-1430.
- [17] Z. Zhang and S. Dian, "Motion Control of Manipulators Based on Model-free Adaptive Control," in *2018 3rd International Conference on Automation, Control and Robotics Engineering*, 2018.
- [18] X. Guo *et al.*, "A Novel Pneumatic Artificial Muscle-driven Robot for Multi-joint Progressive Rehabilitation," in *2018 Joint IEEE 8th International Conference on Development and Learning and Epigenetic Robotics (ICDL-EpiRob)*, 2018, pp. 78-83.
- [19] G. Andrikopoulos, G. Nikolakopoulos, and S. Manesis, "Motion control of a novel robotic wrist exoskeleton via pneumatic muscle actuators," in *2015 IEEE 20th Conference on Emerging Technologies & Factory Automation (ETFA)*, 2015, pp. 1-8.
- [20] S. Jin, Z. Hou, and R. Chi, "Higher-order model-free adaptive control for a class of discrete-time SISO nonlinear systems," in *chinese control and decision conference*, 2011, pp. 2614-2619.